On the relationship between individual cloud entrainment probability density functions and the mean field behavior

Jordan T. Dawe[1] and Philip H. Austin[1]

Corresponding author: P. H. Austin, Department of Earth, Ocean and Atmospheric Sciences, The University of British Columbia, Room 2020, Earth Sciences Building, 2207 Main Mall, Vancouver, British Columbia, V6T 1Z4, Canada. (paustin@eos.ubc.ca)

[1]Department of Earth, Ocean, and Atmospheric Sciences, University of British Columbia, Canada.

Abstract. We use large eddy simulations of entrainment rates for individual clouds and satellite-measured distributions of cloud size to examine how bulk cloud-field entrainment depends on the details of the cloud size distribution. Under the assumption that cloud entrainment is inversely proportional to cloud radius, we find that the dependence of bulk cloud field entrainment on mean cloud area depends strongly on the exponent of the power-law distribution of cloud sizes. For power law exponents corresponding to observed cloud fields we find the bulk entrainment rate is inversely proportional to the length scale of the largest clouds in the field.

1. Introduction

Work on laboratory water tank experiments of turbulent thermal plumes [*Turner*, 1963] indicates such plumes entrain mass as they rise according to

$$\frac{1}{M}\frac{\partial M}{\partial z} = \frac{E}{M} = \epsilon \approx \frac{0.2}{R} \tag{1}$$

where $M = \rho w a$ ($\mathrm{kg\,s^{-1}}$) is the upward mass flux of the plume, ρ is the density of the fluid ($\mathrm{kg\,m^{-3}}$), w is the vertical velocity of the fluid ($\mathrm{m\,s^{-1}}$), a is the area of the plume ($\mathrm{m^2}$), E is the rate at which the cloud entrains mass per unit length of cloud circumference (kg $\mathrm{m^{-1}\ s^{-1}}$), ϵ is the fractional entrainment rate ($\mathrm{m^{-1}}$), and R is the radius of the plume (m). Many parameterizations of cumulus cloud fields use this functional form for the entrainment rate of the cloud field, with R taken as an average updraft size [*Tiedtke*, 1989; *Kain and Fritsch*, 1990; *Kain*, 2004] or the boundary layer depth [*Bretherton et al.*, 2004]. Implicit in these parameterizations is the assumption that the relationship between updraft radius and entrainment rate for an individual cloud plume can be applied to a cloud field composed of clouds of many different sizes. This assumption is made explicitly in the recent study by *Stirling and Stratton*, which features a plot comparing the bulk entrainment rate of a cloud field to the inverse of the square root of the mean area of the clouds in the field [Fig. 13, *Stirling and Stratton*, 2012].

That many authors over several decades have assumed an inverse relationship exists between the bulk entrainment rate and some characteristic length scale of the cloud field attests to this idea's intuitive appeal. However, there is no *a priori* reason this relationship should hold. That the bulk entrainment rate of the cloud field decreases with increasing cloud area is uncontroversial, having been verified in model simulations using both tracer

budgets [*Stirling and Stratton*, 2012] and direct entrainment calculations [*Romps*, 2010]. However, the true relationship between the bulk entrainment rate of the cloud field and the mean cloud area should depend on both the variation of entrainment rate with cloud size and the distribution of cloud sizes in the cloud field.

It is well established from photos taken by airplane and satellite that cumulus cloud size distributions follow a power law relationship [*Benner and Curry*, 1998; *Cahalan and Joseph*, 1989; *Sengupta et al.*, 1990; *Kuo et al.*, 1993; *Neggers et al.*, 2003a, b; *Rodts et al.*, 2003; *Zhao and Girolamo*, 2007; *Gryschka et al.*, 2008; *Jiang et al.*, 2008] of the form

$$n(l) = n_0 l^{-b} \tag{2}$$

where l is the cloud length scale (m), generally calculated as the square root of the cloud horizontal area, $n(l)dl$ is the number of clouds with horizontal length scales between l and $l + dl$, b is a dimensionless parameter which determines the relative proportion of large to small clouds, and n_0 (units of m^b) is a parameter which depends upon the total cloud fraction. Many studies find that a scale break exists between $l_s = 500$–$1300\,\mathrm{m}$ [*Benner and Curry*, 1998; *Neggers et al.*, 2003a, b], but it is unclear if this is an artifact of the curve-fitting technique used [*Zhao and Girolamo*, 2007]. The power law relationship appears to vary with time and location; values for b ranging from 0.636 [*Benner and Curry*, 1998] to ≈ 4 [*Sengupta et al.*, 1990] have been reported in the literature, with the majority of values falling between 1.7–2.3 [*Benner and Curry*, 1998; *Neggers et al.*, 2003a, b; *Zhao and Girolamo*, 2007].

On the other hand, few studies have examined the variation of entrainment rate with cloud size for individual clouds. *Dawe and Austin* [2012] found the entrainment rates of individual clouds showed little dependence on cloud area in large eddy simulations of

shallow cumulus. However, this finding seems to contradict the observed dependence of bulk entrainment rates on cloud size found in simulations of large clouds [*Romps*, 2010; *Stirling and Stratton*, 2012], possibly indicating that the dependence of entrainment on area changes between shallow and deep convection.

In this paper we perform a theoretical examination of the dependence of bulk entrainment rate on the exact forms of the cloud distribution and the relationship between individual cloud entrainment rate and cloud length scale. Section 2 examines the dependence of bulk entrainment rate on the distribution of cloud size, vertical mass flux, and mass entrainment rate. Section 3 examines how altering the relationship between entrainment and length scale for individual clouds affects the bulk entrainment rate. Finally, we present our conclusions in section 4.

2. Theoretical Framework

Given a distribution of cloud sizes $n(l) = n_0 l^{-b}$, the bulk cloud field fractional entrainment rate $\overline{\epsilon}$ (m^{-1}) can be calculated from the entrainment rate distribution $E(l)$ (kg s^{-1} m^{-1}) and vertical mass flux distribution $M(l)$ (kg s^{-1}) of individual clouds via

$$\overline{\epsilon} = \frac{\int E(l)n(l)dl}{\int M(l)n(l)dl} \tag{3}$$

where $\overline{\epsilon}$ is the bulk fractional entrainment rate of the cloud field (m^{-1}), and the integrals are taken over the entire range of cloud field length scales. To examine the dependence of $\overline{\epsilon}$ therefore requires an understanding of the dependence of $E(l)$ and $M(l)$ as well as $n(l)$.

We assume the distribution of fractional entrainment rate with cloud length scale for individual cumulus clouds takes the form

$$\epsilon(l) = \epsilon_0 l^{-e}, \tag{4}$$

where ϵ_0 is a constant with units of m^{e-1}. The exponent $(-e)$ is assumed to be negative since modeling studies have established that bulk fractional entrainment rates decrease as a cloud field transitions from shallow to deep convection [*Romps*, 2010; *Stirling and Stratton*, 2012], and it is difficult to see how this would occur if individual clouds entrainment rates did not decrease with increasing length scale.

Similarly, we assume the distribution $M(l)$ follows a relationship of the form

$$M(l) = M_0 l^m, \tag{5}$$

where M_0 is a constant with units of kg s^{-1} m^{-m}. The exponent m is assumed to be positive as larger clouds tend to carry more vertical mass flux than smaller clouds [*Khairoutdinov and Randall*, 2006; *Stirling and Stratton*, 2012; *Dawe and Austin*, 2012].

Using the relationship $E = \epsilon M$ with equations (4) and (5) results in the distribution of E with cloud size

$$E(l) = \epsilon(l) M(l) = E_0 l^{(m-e)}, \tag{6}$$

where $E_0 = \epsilon_0 M_0$.

Combining equations (2), (5) and (6) with (3), we find the bulk fractional entrainment rate of the cloud field is then given by

$$\overline{\epsilon} = \frac{\int E(l) n(l) dl}{\int M(l) n(l) dl} = \epsilon_0 \frac{\int l^{(m-b-e)} dl}{\int l^{(m-b)} dl}. \tag{7}$$

Note that in the trivial case where $\epsilon(l)$ is independent of cloud length scale ($e = 0$), the bulk fractional entrainment rate will simply be the fractional entrainment rate of the individual clouds, ϵ_0.

3. Parameter ranges for b, m, and e

Now we turn to the question of what ranges of values are valid for the exponents b, m and e of the cloud property distributions. As remarked in the introduction, values of the power law parameter b in equation (2) have been measured ranging from 0.636 to $\approx$ 4, with the majority of values falling between 1.7–2.3 [*Benner and Curry*, 1998; *Neggers et al.*, 2003a, b; *Zhao and Girolamo*, 2007]. On the other hand, the distributions of E and M with cloud length scale l have not been widely evaluated for shallow cumulus in the literature.

To examine $M(l)$ and $E(l)$ we turn to Large Eddy Simulation (LES) output from two standard Global Energy and Water Cycle Experiment (GEWEX) Cloud System Studies (GCSS) Barbados Oceanographic and Meteorological Experiment [BOMEX; *Siebesma et al.*, 2003] and Atmospheric Radiation Measurement Study [ARM; *Brown et al.*, 2002] runs. All LES calculations in this paper were made using the System for Atmospheric Modelling [SAM version 6.8.2; *Khairoutdinov and Randall*, 2003]. Full details of these simulations can be found in *Dawe and Austin* [2012]. Values of M, E and a were found for the cloud core (defined as cloudy, upward moving, buoyant gridcells) of each cloud at each simulated height at one minute intervals and used to examine the dependence of these properties on cloud length scale.

We fit equations of the form $M = M_0 l^m$ to the LES values of M and l (Figure 1). Taking the log of both sides of the mass flux distribution gives $\log_{10}(M) = \log_{10}(M_0) + m \log_{10}(l)$, so m can be found as the slope of the best-fit line between $\log_{10}(M)$ and $\log_{10}(l)$. Performing this fit on the combined LES output from every height results in m = 2.37 for both the BOMEX (Figure 1a) and ARM (Figure 1b) models. If instead we

perform these fits at each model height at 50 metre intervals, we find m takes on values between $m = 2$ and 2.5 (Figure 1c-d).

Instead of fitting $\epsilon(l)$ directly, we instead fit $E = E_0 l^{m-e}$ to the LES values of E and l to find $m - e$, and then subtract this from the previously determined m values to find e. Fitting E instead of ϵ has the advantage that E goes to zero as l goes to zero (Figure 2a-b), while ϵ becomes noisy as l goes to zero as it is measured as the ratio of two small quantities, E/M. Performing this fit on the LES output from all heights produces $m - e$ = 2.54, e = -0.17 for BOMEX and $m - e = 2.15$, $e = 0.22$ for ARM. Performing these fits at each model height at 50 metre intervals we find e has values ranging between -0.4 and 0.6, with the BOMEX values clustering around -0.1 and the ARM values between 0.1 and 0.4 (Figure 2c-d).

4. Dependence of $\overline{\epsilon}$ on largest cloud size and mean cloud area

The integrals in (7) are divergent if performed from 0 to ∞. Instead we perform the integrals between two length scales l_1 and l_2, which represent the size of the smallest and largest clouds in the cloud field, respectively. This results in

$$\overline{\epsilon} = \epsilon_0 \frac{\int_{l_1}^{l_2} l^{m-b-e} dl}{\int_{l_1}^{l_2} l^{m-b} dl} = \epsilon_0 \left(\frac{1+m-b}{1+m-b-e} \right) \left[\frac{l_2^{(1+m-b-e)} - l_1^{(1+m-b-e)}}{l_2^{(1+m-b)} - l_1^{(1+m-b)}} \right]. \tag{8}$$

With representative values of b, m, and e in hand we now turn to the question of the dependence of $\overline{\epsilon}$ on l_2 and $\overline{a}$.

For the purposes of this paper we set l_1 to 10 m, which seems a reasonable minimum scale for a turbulent cumulus cloud. Our calculations indicate that variations in l_1 between 1 m and 100 m have relatively little effect on the bulk entrainment rate (at most, a factor

of 2) for observed values of b and values of $l_2 \geq 1000\,\mathrm{m}$. With l_1 fixed we are effectively left with three free variables: l_2, $(m-b)$, and e.

If we take $m = 2.25$, b=1.75, and e=0.25 to be representative values, $(1+m-b)$ and $(1+m-b-e)$ are both positive terms and, since $l_2 \gg l_1$, (8) reduces to

$$\overline{\epsilon} \approx \epsilon_0 \left(\frac{1+m-b}{1+m-b-e} \right) l_2^{-e}. \tag{9}$$

Thus we find the bulk fractional entrainment of the cloud field varies in the same manner as the fractional entrainment rate of the individual clouds in the field, with the cloud size replaced with the size of the largest clouds in the field.

Stirling and Stratton [2012] use the mean area per cloud as the relevant length scale for predicting the bulk entrainment rate of the cloud field. To see how well this variable performs as a parameterization of the bulk entrainment, we calculate the mean area per cloud of the cloud field (m^2),

$$\overline{a} = \frac{\int a n(l) dl}{\int n(l) dl} \tag{10}$$

Substituting equation (2) into (10) and integrating from l_1 to l_2 results in

$$\overline{a} = \frac{\int_{l_1}^{l_2} l^{(2-b)} dl}{\int_{l_1}^{l_2} l^{-b} dl} = \left(\frac{1-b}{3-b} \right) \left[\frac{l_2^{(3-b)} - l_1^{(3-b)}}{l_2^{(1-b)} - l_1^{(1-b)}} \right]. \tag{11}$$

If we again take b=1.75 as a representative value for the cloud size distribution parameter, we find that for $l_2 \gg l_1$ (11) reduces to

$$\overline{a} \approx \left(\frac{1-b}{3-b} \right) \left[\frac{l_2^{(3-b)}}{l_1^{(1-b)}} \right] \tag{12}$$

Rearranging this and substituting into equation (9) we find

$$\overline{\epsilon} \approx \epsilon_0 \left(\frac{1+m-b}{1+m-b-e} \right) \left(\frac{3-b}{1-b} \right)^{-e/(3-b)} \left[\frac{\overline{a}}{l_1^{(b-1)}} \right]^{-e/(3-b)}. \tag{13}$$

This result is close to the assumption made by *Stirling and Stratton* [2012] that $\overline{\epsilon} \propto \overline{a}^{-e/2}$, but has an extra dependence on the value of b.

To examine the validity of these approximations we plot equation (8) against l_2 and $\overline{a}$ for a range of m and b values (Fig. 3). (We set $e = 1$ for most of these calculations as changes in e simply alter the resulting relationships proportionally and have little effect on our conclusions.) For positive values of $(m-b)$, $\overline{\epsilon}$ indeed appears to follow a ${l_2}^{-e}$ relationship. However, negative values of $(m-b)$ cause increasing divergence from this relationship in a manner that causes $\overline{\epsilon}$ to be underpredicted by ${l_2}^{-e}$. Conversely, for values of b less than one $\overline{\epsilon}$ follows a $\overline{a}^{-e/2}$ relationship, while larger values of b cause $\overline{\epsilon}$ to be overpredicted by $\overline{a}^{-e/2}$.

We quantify this behaviour by sampling values of equation (8) over a range of logarithmically spaced values of l_2 and $\overline{a}$ with $e = 1$, $m = 2$, over a variety of values of b, then finding least-squared best-fit lines between the logarithm of these values and $\log(\overline{\epsilon})$; the slope of these best fit lines will be the best-fit power-law relationship between the variables. Our results are summarized in Table 1. The power-law relationship exponent between $\overline{\epsilon}$ and l_2 is within 5% of ${l_2}^{-e}$ for values of $m-b$ over 0.5. On the other hand, the power-law relationship exponent between $\overline{\epsilon}$ and $\overline{a}$ is within 5% of $\overline{a}^{-e/2}$ only for values of b less than 0.5. For realistic values of m and b, ${l_2}^{-e}$ is a much more accurate parameterization of $\overline{\epsilon}$ than $\overline{a}^{-e/2}$.

5. Variation in ϵ due to cloud distribution

Finally, we examine the variation in the range of the bulk entrainment values implied by the cloud distributions observed by *Benner and Curry* [1998] and *Zhao and Girolamo* [2007]. *Benner and Curry* fit a double power-law relationship to the satellite-observed

cloud area distribution, with the power-law exponent abruptly changing at some scale break length so that the power-law exponent is smaller for large clouds than for small clouds. However, *Zhao and Girolamo* question the validity of these double power-law fits, since large clouds can be easily under-sampled in cloud field snapshots. For simplicity, instead of performing bulk entrainment rate calculations for a double power-law relationship, we simply use the power-law relationship fit for small clouds and use the scale break length as a proxy for the size of the largest clouds in the cloud field. While this cannot be considered an accurate estimate of these length parameters, it should provide an indication of the range of variation in $\bar{\epsilon}$ due to variations in the cloud size distribution.

We set $m = 2.25$ and $e = 0.2$ and plot the variation in $\bar{\epsilon}$ versus b and l_2 across the range of observed shallow cumulus distributions (Fig. 4). Bulk fractional entrainment rate appears to depend primarily on l_2, with a milder dependence on b appearing as the maximum cloud size increases. (Performing this calculation with $e = 1$ shows a much stronger dependence on b relative to l_2—as cloud length scale becomes more important to entrainment, the distribution of cloud length scales has more effect.) We see that even with this mild dependence between ϵ and l, $\bar{\epsilon}/\epsilon_0$ varies between ≈ 0.27–0.375 over the range of observed cloud distribution parameters.

6. Conclusions

We have used satellite-derived cloud size distributions and LES-derived relationships between entrainment and cloud size to investigate the relationship between cloud size and bulk fractional entrainment rate of a shallow cloud field. For ensembles of BOMEX and ARM LES clouds, we find the vertical mass flux $M(l)$ and fractional entrainment rate $\epsilon(l)$

of individual shallow cumulus follow power-law relationships with exponents in the range m = 2–2.5 for mass flux and e = -0.1–0.4 for fractional entrainment rate.

Comparing the dependences of $\overline{\epsilon}$ on l_2 and $\overline{a}$ shows that l_2^{-e} is a reasonable proxy for $\overline{\epsilon}$ for values of $(m-b)$ larger than 0, while $\overline{a}^{-e/2}$ is a reasonable proxy for $\overline{\epsilon}$ at values of b less than 1. However, as b increases, the relationships between l_2, $\overline{a}$ and $\overline{\epsilon}$ increasingly diverge from these approximations. In general, the l_2^{-e} approximation overestimates the dependence of $\overline{\epsilon}$ on l_2, while $\overline{a}^{-e/2}$ underestimates the dependence of $\overline{\epsilon}$ on $\overline{a}$. Of these two measures of $\overline{\epsilon}$, l_2^{-e} diverges slower and is simpler to calculate, indicating that the size of the largest clouds in the field provides a better proxy for bulk entrainment rate than the mean area per cloud.

Large scale parameterizations of cloud entrainment began with insights obtained from single entraining plumes. The ability of large eddy simulations to determine entrainment for a broad range of cloud sizes allows us to examine the role that cloud size plays in setting the bulk entrainment rate for a realistic size distribution of shallow clouds. Our results suggest that the cloud size distribution and the dependence of entrainment rate on cloud size may have important effects on the bulk entrainment rate of a cloud ensemble. However, including these effects in cloud parameterizations will require improving our understanding of the processes that determine the cloud size distribution.

Acknowledgments. Support for this research was provided by the Canadian Foundation for Climate and Atmospheric Science through the Cloud Aerosol Feedback and Climate network. Figures were generated using the matplotlib library [*Hunter*, 2007] in the Python programming language.

References

Benner, T. C., and J. A. Curry (1998), Characteristics of small tropical cumulus clouds and their impact on the environment, *J. Geophys. Res.-Atmos.*, *103*, 28,753–28,767.

Bretherton, C. S., J. R. McCaa, and H. Grenier (2004), A new parameterization for shallow cumulus convection and its application to marine subtropical cloud-topped boundary layers. part i: description and 1d results., *Mon. Wea. Rev.*, *132*, 864–882, doi:10.1175/1520-0493(2004)132¡0883:ANPFSC¿2.0.CO;2.

Brown, A. R., R. T. Cederwall, A. Chlond, P. G. Duynkerke, J.-C. Golaz, M. F. Khairoutdinov, D. C. Lewellen, A. P. Lock, M. K. Macvean, C.-H. Moeng, R. A. J. Neggers, A. P. Siebesma, and B. Stevens (2002), Large-eddy simulation of the diurnal cycle of shallow cumulus convection over land, *Q. J. R. Meteorol. Soc.*, *128*, 1075–1093, doi:10.1256/003590002320373210.

Cahalan, R. F., and J. H. Joseph (1989), Fractal statistics of cloud fields, *Mon. Wea. Rev.*, *117*, 261–272.

Dawe, J. T., and P. H. Austin (2012), Statistical analysis of an les shallow cumulus cloud ensemble using a cloud tracking algorithm, *Atmospheric Chemistry and Physics*, *12*, 1101–1119, doi:10.5194/acp-12-1101-2012.

Gryschka, M., B. Witha, and D. Etling (2008), Scale analysis of convective clouds, *Meteorologische Zeitschrift*, *17*, 785–791.

Hunter, J. D. (2007), Matplotlib: A 2d graphics environment, *Comput. Sci. Eng.*, *9*(3), 90–95, doi:10.1109/MCSE.2007.55.

Jiang, H., G. Feingold, H. H. Jonsson, M.-L. Lu, P. Y. Chuang, R. C. Flagan, and J. H. Seinfeld (2008), Statistical comparison of properties of simulated and observed cumulus

clouds in the vicinity of Houston during the Gulf of Mexico Atmospheric Composition and Climate Study (GoMACCS), *J. Geophys. Res.-Atmos.*, *113*, D13,205, doi: 10.1029/2007JD009304.

Kain, J. S. (2004), The kainfritsch convective parameterization: An update, *J. Appl. Meteor.*, *43*(1), 170–181.

Kain, J. S., and J. M. Fritsch (1990), A one-dimensional entraining/detraining plume model and its application in convective parameterization, *J. Atmos. Sci.*, *47*, 2784–2802.

Khairoutdinov, M., and D. Randall (2006), High-resolution simulation of shallow-to-deep convection transition over land, *J. Atmos. Sci.*, *63*, 3421–3436.

Khairoutdinov, M. F., and D. A. Randall (2003), Cloud resolving modeling of the arm summer 1997 iop: model formulation, results, uncertainties, and sensitivities, *J. Atmos. Sci.*, *60*, 607–625.

Kuo, K.-S., R. M. Welch, R. C. Weger, M. A. Engelstad, and S. K. Sengupta (1993), The three-dimensional structure of cumulus clouds over the ocean: 1. structural analysis, *J. Geophys. Res.-Atmos.*, *98(D11)*, 20,685–20,711, doi:10.1029/93JD02331.

Neggers, R. A. J., H. J. J. Jonker, and A. P. Siebesma (2003a), Size statistics of cumulus cloud populations in large-eddy simulations, *J. Atmos. Sci.*, *60*, 1060–1074.

Neggers, R. A. J., P. G. Duynkerke, and S. M. A. Rodts (2003b), Shallow cumulus convection: a validation of large-eddy simulation against aircraft and Landsat observations, *Q. J. R. Meteorol. Soc.*, *129*, 2671–2696.

Rodts, S. M. A., P. G. Duynkerke, and H. J. J. Jonker (2003), Size distributions and dynamical properties of shallow cumulus clouds from aircraft observations and satellite

data, *J. Atmos. Sci.*, *60*, 1895–1912.

Romps, D. M. (2010), A direct measure of entrainment, *J. Atmos. Sci.*, *67*(6), 1908–1927.

Sengupta, S. K., R. M. Welch, M. S. Navar, T. A. Berendes, and D. W. Chen (1990), Cumulus cloud field morphology and spatial patterns derived from high spatial resolution landsat imagery, *Journal of Applied Meteorology*, *29*, 1245–1267.

Siebesma, A. P., C. S. Bretherton, A. Brown, A. Chlond, J. Cuxart, P. G. Duynkerke, H. Jiang, M. Khairoutdinov, D. Lewellen, C.-H. Moeng, E. Sanchez, B. Stevens, and D. E. Stevens (2003), A large eddy simulation intercomparison study of shallow cumulus convection, *J. Atmos. Sci.*, *60*, 1201–1219, doi:10.1175/1520-0469(2003)60¡1201:ALESIS¿2.0.CO;2.

Stirling, A. J., and R. A. Stratton (2012), Entrainment processes in the diurnal cycle of deep convection over land, *Q.J.R. Meteorol. Soc.*, *138*, 1135–1149, doi:10.1002/qj.1868.

Tiedtke, M. (1989), A comprehensive mass flux scheme for cumulus parameterization in large-scale models, *Mon. Wea. Rev.*, *117*, 1779–1800.

Turner, J. S. (1963), The motion of buoyant elements in turbulent surroundings, *Journal of Fluid Mechanics*, *16*, 1–16.

Zhao, G., and L. D. Girolamo (2007), Statistics on the macrophysical properties of trade wind cumuli over the tropical western atlantic, *J. Geophys. Res.-Atmos.*, *112*, D10,204, doi:10.1029/2006JD007371.

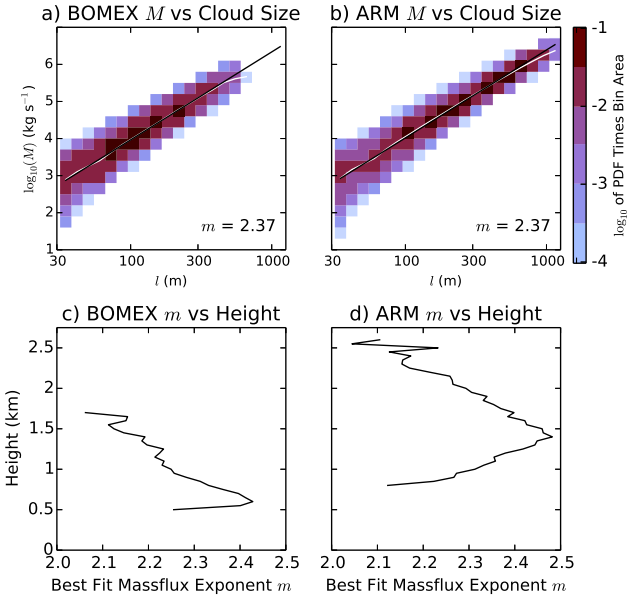

Figure 1. Powerlaw fits for vertical mass flux M versus cloud length scale l. a) and c) are calculated from a BOMEX LES and b) and d) from an ARM LES. a) and b) show fits based upon data from all heights; white lines show mean M at each l, black lines show the best-fit powerlaw. c) and d) show powerlaw fit exponent m as a function of height in 50 meter bins.

Table 1. Best fit power law exponents between l_2 and $\overline{\epsilon}$ and $\overline{a}$ and $\overline{\epsilon}$ for a variety of values of e, m, and b.

e	m	b	$m-b$	$\overline{\epsilon}$ vs l_2	$\overline{\epsilon}$ vs $\overline{a}$
1	2	0.5	1.5	0.998	0.521
		1	1	0.992	0.552
		1.5	0.5	0.960	0.646
		2	0	0.822	0.773
		2.5	-0.5	0.500	0.842
0.5		1.5	0.5	0.472	0.335

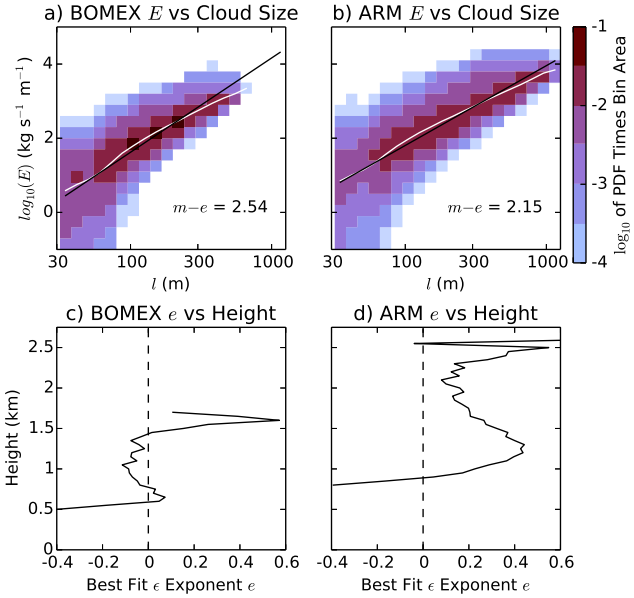

Figure 2. Powerlaw fits for mass entrainment E versus cloud length scale l. a) and c) are calculated from a BOMEX LES and b) and d) from an ARM LES. a) and b) show fits based upon data from all heights; white lines show mean E at each l, black lines show the best-fit powerlaw. c) and d) show fractional entrainment rate powerlaw fit exponent e as a function of height in 50 meter bins.

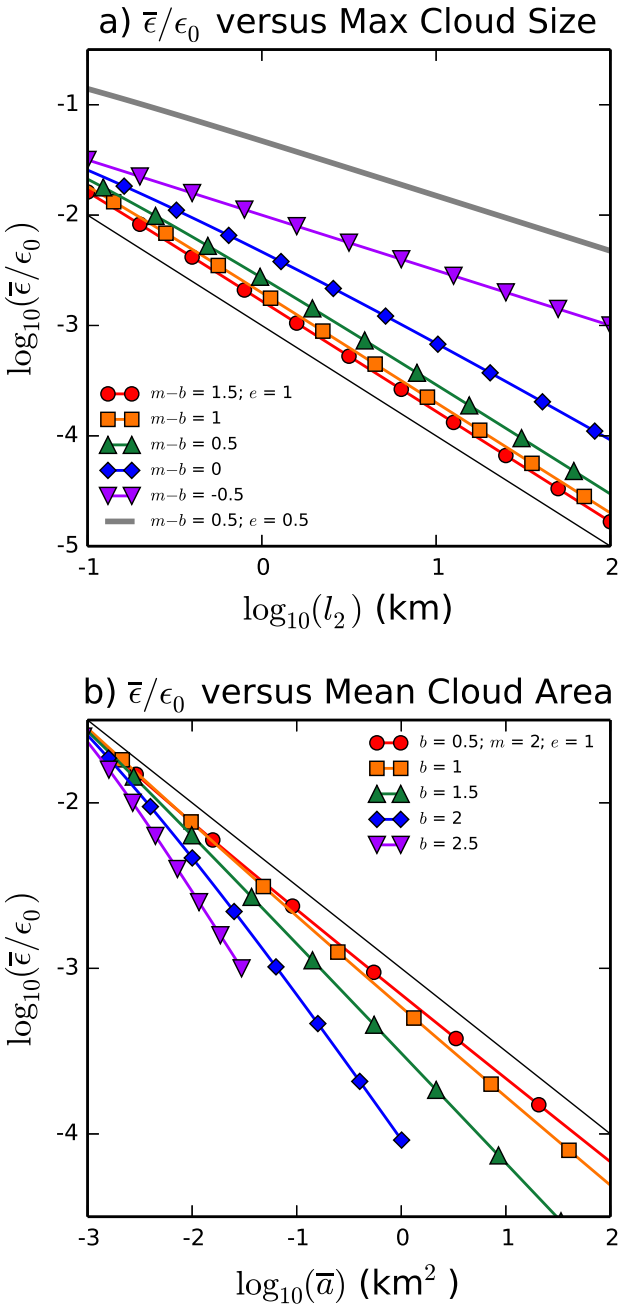

Figure 3. Dependence of the bulk cloud plume entrainment rate $\overline{\epsilon}$ on a) the length scale of the largest clouds in the cloud field l_2 and b) the mean cloud area $\overline{a}$ for various values of the size distribution power-law exponent b. Thin grey lines show a) ${l_2}^{-1}$ or b) $\overline{a}^{-1/2}$ relationships.

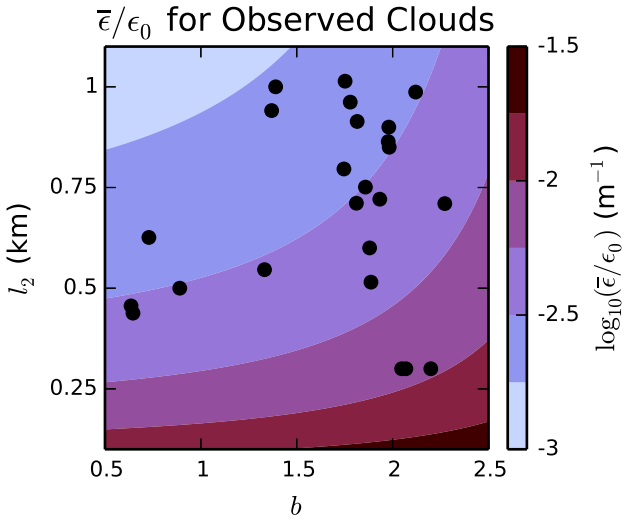

Figure 4. Bulk cloud plume entrainment rate $\overline{\epsilon}$ for various values of the power-law size distribution exponent b and maximum cloud size l_2, assuming $\epsilon \propto l^{-0.2}$. Dots indicate the observational b and l_2 values inferred from *Benner and Curry* [1998] and *Zhao and Girolamo* [2007].